

Showcasing research from the McNeil laboratory at the University of Michigan.

Title: Impact of π -Conjugated Gradient Sequence Copolymers on Polymer Blend Morphology

Novel gradient sequence π -conjugated copolymers were compared to analogous random and block copolymers. Gradient copolymers were especially useful as additives to control the morphology and domain size in homopolymer blends, which should impact future bulk heterojunction solar cell designs.

As featured in:



See E. F. Palermo *et al.*,
Polym. Chem., 2013, **4**, 4606.

RSC Publishing

www.rsc.org/polymers

Registered Charity Number 207890

Impact of π -conjugated gradient sequence copolymers on polymer blend morphology†

Cite this: *Polym. Chem.*, 2013, **4**, 4606

Edmund F. Palermo,^{*} Harry L. van der Laan and Anne J. McNeil^{*}

A gradient sequence copolymer containing 3-hexylthiophene (3HT) and 3-(6-bromohexyl)thiophene (3BrHT) with a linear change in comonomer composition was synthesized *via* a controlled, chain-growth semi-batch method. For comparison, random and block copolymers with the same molecular weight and comonomer ratio (1 : 1) were prepared. All three copolymers exhibited similar molecular weight ($M_n \sim 32$ kDa), low dispersity ($\mathcal{D} < 1.2$) and high regioregularity (>99%), suggesting that any differences among the three copolymers can be attributed to the different copolymer sequences. The optical and thermal properties, as well as the thin film morphologies, of the gradient copolymer were compared to the random and block copolymers and the physical blend of the homopolymers. The physical blends showed extensive micron-scale phase separation by AFM and TEM. Adding the gradient copolymer to the blend resulted in a dramatic reduction in the domain size. Moreover, the domain size decreased as the amount of the gradient copolymer increased, suggesting that the copolymer is compatibilizing the polymer blend. By comparison, the random and block copolymers were less effective compatibilizing agents, which indicates that the gradient sequence copolymer is well suited to tailor the morphology of immiscible polymer blends.

Received 10th May 2013
Accepted 27th June 2013

DOI: 10.1039/c3py00601h

www.rsc.org/polymers

Introduction

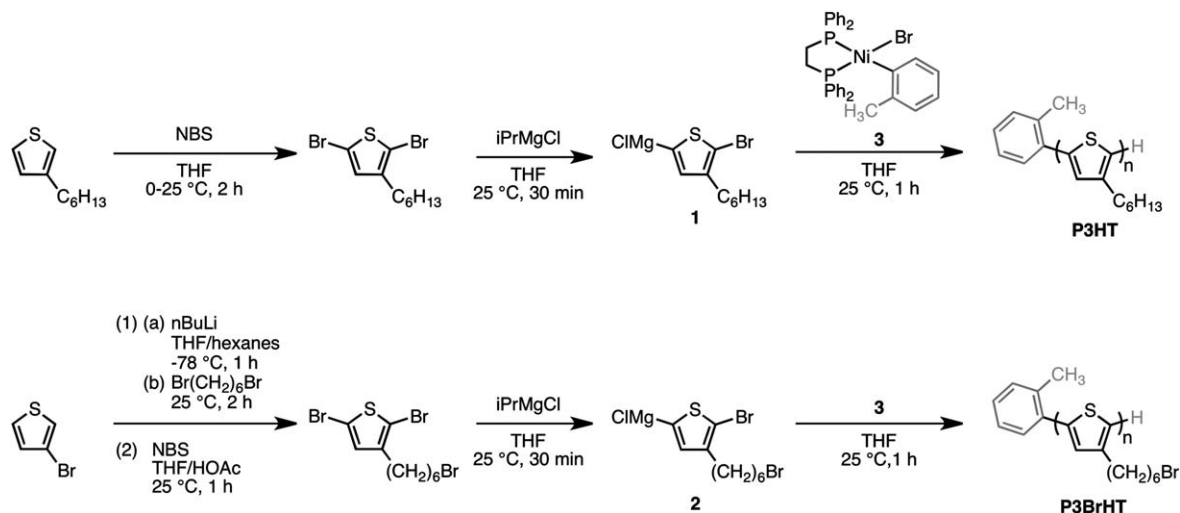
One of the grand challenges in polymer science is the ability to synthesize polymers with control over the comonomer sequence.¹ Inspired by the precise sequence control exhibited in biomolecule synthesis, the rationale for sequence control in synthetic polymers is simple: a wide variety of properties might be accessible from a few monomers. Although this type of control remains challenging for non-natural polymers, several copolymer sequences can be accessed using chain-growth polymerizations (*e.g.*, alternating, block and gradient). Of these, block copolymers are the most extensively studied,^{2,3} whereas gradient copolymers are relatively new.^{4,5} Nonetheless, gradient copolymers have exhibited unique properties, such as compatibilizing phase-separated blends of two different homopolymers.⁶ This result has been attributed to the copolymer localizing at the polymer–polymer interface and lowering the interfacial tension, which reduces domain sizes and renders the blend thermally stable. While this phenomenon is known for amorphous gradient copolymers, there are no reports on the effect of semicrystalline gradient copolymers on blend morphology.

Because phase separation significantly impacts the performance of bulk heterojunction (BHJ) solar cells,⁷ π -conjugated gradient copolymers may provide a new route for controlling blend morphology. Specifically, we hypothesized that these copolymers might mediate the crystallization process from solution and lead to unique morphologies. To test this hypothesis, we selected a pair of thiophene comonomers which differ only in their side chain identity: 3-hexylthiophene (3HT) and 3-(6-bromohexyl)thiophene (3BrHT). The bulky bromine substituent is expected to disrupt the close packing of these side-chains, giving the brominated polymer a subtly different solid-state structure while retaining its semicrystallinity.⁸ Polythiophenes were specifically targeted because they have shown promise as the active components in BHJ solar cells⁹ and can be polymerized in a controlled chain-growth fashion using the recently developed catalyst transfer polycondensation (CTP).^{10–12} CTP has enabled access to novel conjugated materials, including block and gradient copolymers,^{3,5} star polymers,¹³ and surface-grafted polymers.¹⁴

We describe herein the synthesis and characterization of three copolymers (gradient, block, random) containing an equimolar ratio of the two monomers, as well as the corresponding homopolymers. As anticipated, the bromine substituent alters the solid-state structure of the homopolymers, leading to a phase-separated polymer blend with micron-scale domains. Adding each copolymer to the blend resulted in reduced domain sizes. The gradient copolymer provided the largest reduction, suggesting that a gradient sequence is most

Department of Chemistry and Macromolecular Science and Engineering Program, University of Michigan, 930 North University Avenue, Ann Arbor, Michigan 48109-1055, USA. E-mail: ajmcneil@umich.edu

† Electronic supplementary information (ESI) available: Materials and methods, synthetic procedures and characterization data. See DOI: 10.1039/c3py00601h



Scheme 1 Monomer and homopolymer synthesis.

effective for controlling the blend morphology of semi-crystalline homopolymers.

Experimental

Detailed procedures and full characterization data can be found in the ESI.†

Results and discussion

Monomer and catalyst synthesis

The monomer syntheses are highlighted in Scheme 1. (5-Bromo-4-hexylthiophen-2-yl)magnesium chloride (**1**) was synthesized following our reported procedure.⁵ (5-Bromo-4-(6-bromohexyl)thiophen-2-yl)magnesium chloride (**2**) was synthesized *via* a modified literature protocol.¹⁵ Lithium-halogen exchange between 3-bromothiophene and *n*BuLi afforded the 3-lithiated thiophene (as a white precipitate)¹⁶ and 1-bromobutane. The supernatant, which contains the 1-bromobutane, was removed *via* cannula transfer and replaced with fresh solvent. Then excess 1,6-dibromohexane was added and the reaction mixture was warmed to room temperature. This procedure leads to higher overall yields by minimizing the side-products resulting from the 1-bromobutane generated in the first step. Subsequent bromination with *N*-bromosuccinimide followed by Grignard metathesis with *i*PrMgCl affords monomer **2**. Toly-functionalized catalyst **3** was synthesized following our reported procedure.^{5a,17}

Homopolymer synthesis and characterization

Poly(3-hexylthiophene) (P3HT) and poly(3-(6-bromohexyl)thiophene) (P3BrHT) were synthesized by chain-growth polymerization using a tolyl-functionalized nickel catalyst (Scheme 1). The tolyl group serves as an end-capping agent to ensure that propagation occurs exclusively from one chain end.¹⁸ MALDI-TOF-MS analysis of oligo-**1** and oligo-**2** synthesized using the same method showed predominately tolyl/H end groups (ESI,

Fig. S12 and S13†),¹⁹ consistent with unidirectional propagation and a controlled, chain-growth polymerization. The number average molecular weight (M_n) increased linearly with conversion and the dispersity (D) remained constant and relatively low (<1.2) throughout the polymerization (ESI, Fig. S9 and S10†), also consistent with a controlled chain-growth polymerization. ¹H NMR spectroscopy revealed that the regioregularity of the homopolymers was greater than 99%, indicating that only the major regioisomer of the Grignard reagent is incorporated into the polymer (ESI, Fig. S7 and S8†).

Thin films of each polymer were spin-cast on glass slides and thermally annealed in a vacuum oven prior to the optical characterization.²⁰ The subtle structural difference (H *versus* Br) between P3HT and P3BrHT had a noticeable impact on the optical properties: the UV-vis spectra showed a prominent absorption associated with H-aggregate formation in P3HT (at 605 nm),²¹ whereas this feature is barely visible in the absorption spectrum of P3BrHT (Fig. 1A). This result suggests that the bulky bromine substituent inhibits these favorable solid-state interactions between the polythiophene chains. Solid-state destabilization is also observed in the differential scanning calorimetry (DSC) thermograms, which showed that P3BrHT

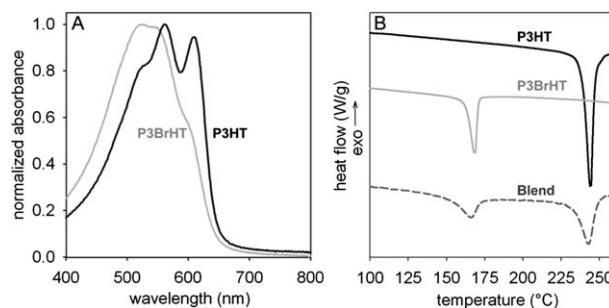


Fig. 1 Homopolymer characterization: (A) UV-vis spectra for thermally annealed thin films of P3HT and P3BrHT. (B) DSC thermograms for P3HT and P3BrHT and the physical blend (1 : 1 v/v).

exhibited a significantly lower melting temperature than P3HT (Fig. 1B). Powder X-ray diffraction (PXRD) analysis confirmed that the two homopolymers exhibited different solid-state structures (ESI, Fig. S21†): the PXRD data for P3HT revealed an interlamellar spacing of 16.7 Å and a π -stacking distance of 3.8 Å, consistent with previous reports.²² In contrast, the interlamellar spacing was not determined for P3BrHT but a π -stacking distance of 4.0 Å was observed. Based on these differences in the solid-state structures, we hypothesized that a physical blend of the two homopolymers might phase separate. Indeed, the DSC thermogram of the physical blend exhibited two distinct melting endotherms, each corresponding to the pristine homopolymers: P3HT ($T_m = 242$ °C) and P3BrHT ($T_m = 168$ °C). This result suggests that the two homopolymers do not cocrystallize into a single phase but rather adopt a phase-separated morphology.

To probe the morphology of the P3HT-P3BrHT blend, thin films were spin-cast from CHCl_3 and analyzed by tapping-mode atomic force microscopy (AFM) without annealing. The phase images revealed a morphology containing globular domains in a continuous matrix (Fig. 2A). We further examined the thin film morphology using transmission electron microscopy (TEM), which is advantageous because it probes the entire film rather than just the surface and the contrast is dependent on the chemical composition. The TEM was also equipped with an energy dispersive spectroscopy (EDS) detector, which is used to determine the elemental composition of selected regions. The scanning mode TEM (STEM) image of the blend using high angle annular dark field detection revealed observable contrast between dark domains in a bright matrix (Fig. 2B). EDS revealed that the dark domains represent P3HT-rich regions whereas the bright matrix represents P3BrHT-rich regions, consistent with a phase-separated thin film (Fig. 2C).

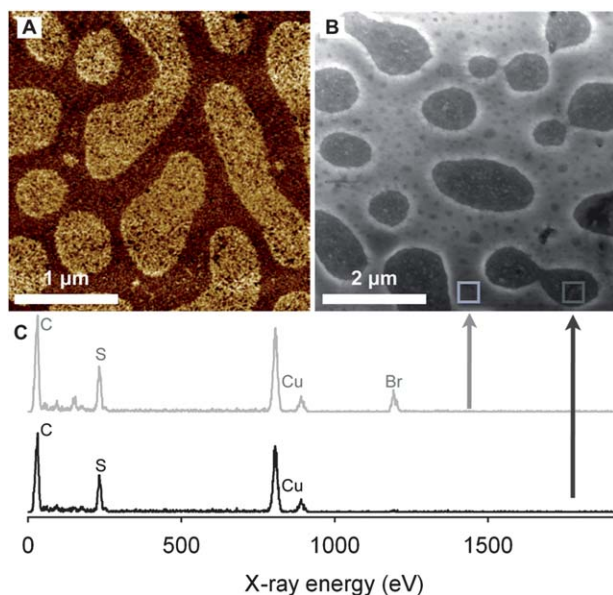


Fig. 2 Blend characterization: (A) AFM phase image and (B) STEM annular dark field image of the P3HT-P3BrHT polymer blend. (C) EDS data for selected regions. (The peaks at ~ 800 eV are from the copper grid used to support the sample.)

Combined, the DSC, AFM, and STEM/EDS data are consistent with micron-scale phase separation in the physical blend of P3HT and P3BrHT. We suspect that the observed phase separation arises from crystallization-induced segregation because it is unlikely that the χN value needed for enthalpy-driven phase separation has been reached based on the similar homopolymer chemical structures and moderate M_n . This blend provides an ideal model system for determining the impact of a gradient copolymer additive on blend morphology.

Copolymer synthesis and characterization

Random and block copolymerizations. Monomers **1** and **2** exhibited similar reactivities in the batch copolymerization (Fig. 3A), which was not surprising considering their similar steric and electronic properties. As a consequence, there was no compositional drift along the polymer backbone, leading to a random sequence copolymer (Fig. 3B). To determine whether the copolymerization was chain-growth and living, several experiments were performed, which included: (i) monitoring the number-average molecular weight (M_n) and dispersity (D) versus conversion (ESI, Fig. S15†), (ii) comparing the observed M_n values to the theoretical M_n based on the initial monomer/catalyst ratio,²³ (iii) performing a sequential monomer addition experiment to make block copolymers (Fig. 3B/C), and (iv) analysing the oligomer end-groups *via* MALDI-TOF-MS (ESI, Fig. S13 and S14†). Combined, these data provided strong evidence of a well-controlled chain-growth polymerization process, which is a prerequisite for synthesizing gradient copolymers.

Gradient copolymerization. Because the monomer reactivities are so similar, the semi-batch method, wherein one

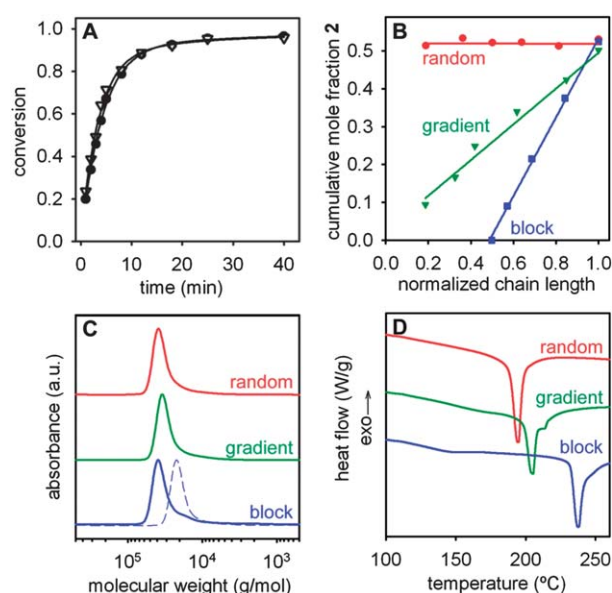


Fig. 3 Copolymer characterization: (A) plot of conversion versus time for the batch copolymerization of **1** (●) and **2** (▽) with catalyst **3**. (B) Plot of the cumulative mole fraction of **2** in the copolymer as a function of normalized chain length. (C) GPC data for the copolymerizations. (Note that the data for both the first (dashed) and second (solid) block is shown.) (D) DSC thermograms for the copolymers.

Table 1 Homopolymer and copolymer characterization data

Polymer	$f_{3\text{BrHT}}$	M_n^a (kDa)	D^a	T_m^b ($^{\circ}\text{C}$)
P3HT	0.00	32.4	1.12	242
P3BrHT	1.00	33.1	1.09	168
Random	0.52	34.7	1.15	198
Gradient	0.50	29.1	1.14	206
Block	0.51	34.4	1.19	146, 235

^a Determined using GPC (calibrated with PS standards) in THF at 40 $^{\circ}\text{C}$.

^b A heating rate of 10 $^{\circ}\text{C min}^{-1}$ was used.

monomer is added over time, is needed to generate a gradient sequence copolymer. Herein, monomer 2 was injected into a flask containing monomer 1 and catalyst 3. To generate a linear gradient sequence copolymer, the addition rate should be similar to the polymerization rate. This addition rate was not feasible at room temperature due to the fast polymerization rate ($\sim 80\%$ conversion within 10 min), but was accessible at 0 $^{\circ}\text{C}$ ($\sim 80\%$ conversion within 60 min). By monitoring the cumulative mole fraction of 2 in the copolymer as a function of normalized chain length, we confirmed that a linear gradient sequence was prepared (Fig. 3B and ESI[†]).

Table 1 provides a summary of the copolymer and homopolymer characterization data. Importantly, each of the synthesized copolymers exhibited similar comonomer compositions ($f_{3\text{BrHT}}$), number-average molecular weights (M_n), and dispersities (D). The salient difference is their sequence distribution, and as a consequence, these copolymers can be used to determine the impact of sequence on properties.

The copolymer sequence had a dramatic effect on the melting processes (Fig. 3D). While both the random and gradient copolymers showed an endotherm that is intermediate between the melting temperatures (T_m) of the corresponding homopolymers, the gradient copolymer exhibited a higher T_m , suggesting that it forms more stable crystallites relative to the random sequence. The gradient copolymer also featured a prominent shoulder peak, suggesting spontaneous melt crystallization.²⁴ The block copolymer, on the other hand, exhibited a broad and weak endotherm at 146 $^{\circ}\text{C}$ as well as a prominent, sharp endotherm at 235 $^{\circ}\text{C}$, which suggests some degree of microphase separation into crystalline domains. Overall, these large differences in thermal properties suggest that the copolymers exhibit markedly different solid-state interactions.

Further insight into the solid-state properties was obtained *via* UV/vis absorption spectroscopy (ESI, Fig. S17 and S18[†]). The spectra for copolymer thin films after thermal annealing²⁵ revealed that each copolymer exhibited a shoulder peak at 600 nm, corresponding to the H-aggregates of the polythiophene backbone.²¹ The relative intensity of these shoulder peaks in the normalized spectra were lower than those in P3HT but greater than those in P3BrHT. This result suggests that the solid-state packing of the copolymers is only partially disrupted by the bulky bromine atoms on 50% of the monomers. Indeed, the PXRD confirmed that each copolymer exhibited reflections consistent with a lamellar structure. The copolymers of P3HT and P3BrHT showed crystallographic reflections at similar

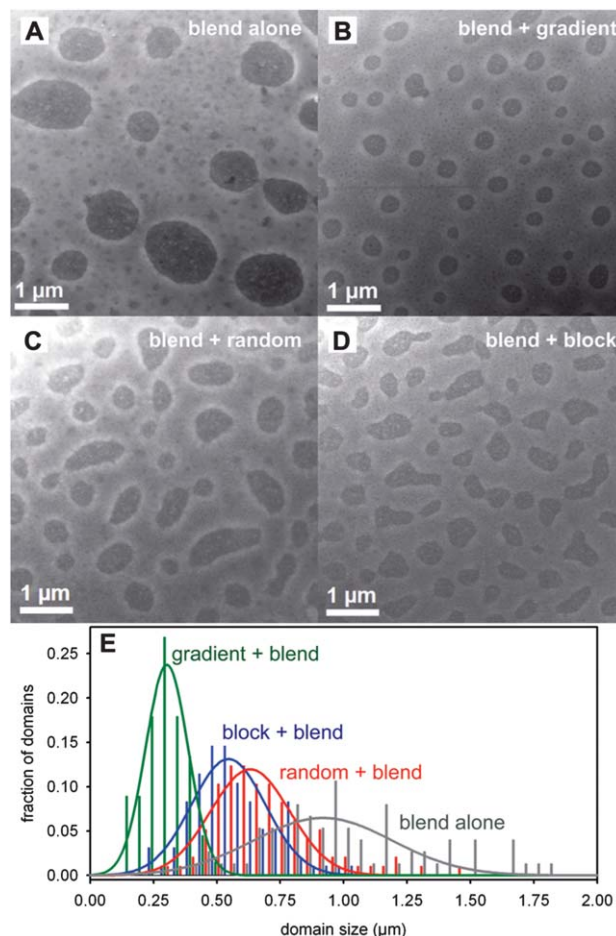


Fig. 4 STEM images of the 1 : 1 (v/v) P3HT-P3BrHT blend (A) without copolymer additive, (B) with 20 wt% gradient copolymer, (C) with 20 wt% random copolymer, (D) with 20 wt% block copolymer. (E) Histogram of the domain size distributions.

positions as the parent homopolymers, suggesting that the solid-state packing structures are closely related for each of these materials. This implies that the presence of $\sim 50\%$ brominated side chains does not significantly disrupt the semicrystalline nature of the copolymers (ESI, Fig. S21[†]).

The morphologies of the annealed copolymer thin films were analyzed by AFM in the tapping mode. While the height images showed relatively smooth surfaces, the phase data provided high-contrast images (ESI, Fig. S25[†]). The random and gradient copolymers formed high-aspect ratio nanowires, whereas the block copolymer formed shorter, worm-like structures. Both of these morphologies are commonly observed in semicrystalline polymers in spin-cast thin films.

P3HT-P3BrHT blends: impact of copolymer additives

The rationale for preparing the random, block and gradient copolymers described herein was to establish the impact of semicrystalline copolymer additives on blend morphology. Whereas the stabilizing influence of gradient copolymer additives on polymer blends is well established for amorphous polymers, the impact of semicrystalline copolymers remains unexplored.

Herein, the morphologies of the as-cast P3HT-P3BrHT blends, with and without copolymer additives, were compared using STEM. Without the copolymer additive, the blend phase separates into P3HT-rich (dark) regions with an average domain size of $0.9 \pm 0.3 \mu\text{m}$ within the P3BrHT-rich (bright) matrix (Fig. 4A). Adding 10 wt% gradient copolymer leads to a dramatic reduction in the P3HT domain size ($0.33 \pm 0.09 \mu\text{m}$).

Increasing the content of gradient copolymer to 20 wt% leads to further reductions in domain size ($0.27 \pm 0.08 \mu\text{m}$, Fig. 4B). Combined, these data provide strong support that the gradient copolymer additive is impacting the crystallization process, presumably through stabilizing interactions at the polymer-polymer interface. For comparison, the random and block copolymers were separately added to the blend at 20 wt% (Fig. 4C and D, respectively). While both copolymers decreased the domain sizes, neither was as effective as the gradient copolymer (Fig. 4E). These data confirm that the gradient sequence is optimal for compatibilizing semicrystalline polymer blends. One rationale for this effect is that the gradient is uniquely capable of simultaneously interacting with the homopolymer phases using its block-like domains, while also modifying the interface using its compositionally varying mid-section.

Conclusions

Conjugated copolymers containing 3HT and 3BrHT with similar M_n , D , and comonomer composition, but varying sequences were synthesized *via* controlled, chain-growth polymerization. Each copolymer exhibited different physical properties, stemming from differences in the solid-state organization. When the copolymers were used as additives in the homopolymer blend, the domain sizes decreased. Overall, the gradient copolymer had the largest impact on domain size, suggesting that the gradient sequence is the most effective for blend compatibilization. We anticipate that these novel materials will have applications in BHJ solar cells, where a key determinant of device performance is the length scale of phase separation. Gradient copolymers can play a key role by tuning the morphology of the all-polymer based devices.²⁶ Before this goal can come to fruition, however, the copolymerization of dissimilar monomers (*e.g.*, donor- and acceptor-based monomers) in a controlled/living fashion must be realized. These and related studies are currently underway in our research laboratories.

Acknowledgements

We thank the Army Research Office (ARO 58200-CH-PCS) for support of this work. A. J. M. thanks the Alfred P. Sloan Foundation and the Camille and Henry Dreyfus Foundation for research fellowships. We also acknowledge funding from NSF grant DMR-9871177 for the TEM instrumentation.

Notes and references

- (a) N. Badi, D. Chan-Seng and J.-F. Lutz, *Macromol. Chem. Phys.*, 2013, **214**, 135–142; (b) J.-F. Lutz, *Polym. Chem.*, 2010, **1**, 55–62; (c) N. Badi and J.-F. Lutz, *Chem. Soc. Rev.*, 2009, **38**, 3383–3390; (d) C. K. Ober, S. Z. D. Cheng, P. T. Hammond, M. Muthukumar, E. Reichmanis, K. L. Wooley and T. P. Lodge, *Macromolecules*, 2009, **42**, 465–471.
- For recent reviews on amorphous block copolymers, see: (a) M. C. Stuparu, A. Khan and C. J. Hawker, *Polym. Chem.*, 2012, **3**, 3033–3044; (b) Y. Mai and A. Eisenberg, *Chem. Soc. Rev.*, 2012, **41**, 5969–5985; (c) M. C. Orilall and U. Wiesner, *Chem. Soc. Rev.*, 2011, **40**, 520–535; (d) H.-C. Kim, S.-M. Park and W. D. Hinsberg, *Chem. Rev.*, 2010, **110**, 146–177.
- For examples of semicrystalline block copolymer synthesis, see: (a) L. Angiolini, A. Brazzi, E. Salatelli, K. Van den Bergh and G. Koeckelberghs, *Macromol. Chem. Phys.*, 2013, **214**, 934–942; (b) M. P. Bhatt, M. K. Huynh, P. Sista, H. Q. Nguyen and M. C. Stefan, *J. Polym. Sci., Part A: Polym. Chem.*, 2012, **50**, 3086–3094; (c) A. G. Sui, X. C. Shi, S. P. Wu, H. K. Tian, Y. H. Geng and F. S. Wang, *Macromolecules*, 2012, **45**, 5436–5443; (d) I. Y. Song, J. Kim, M. J. Im, B. J. Moon and T. Park, *Macromolecules*, 2012, **45**, 5058–5068; (e) L. M. Kozycz, D. Gao, J. Hollinger and D. S. Seferos, *Macromolecules*, 2012, **45**, 5823–5832; (f) J. Hollinger, P. M. DiCarmine, D. Karl and D. S. Seferos, *Macromolecules*, 2012, **45**, 3772–3778.
- For recent examples of amorphous gradient copolymer synthesis, see: (a) J. Chen, J.-J. Li and Z.-H. Luo, *J. Polym. Sci., Part A: Polym. Chem.*, 2013, **51**, 1107–1117; (b) Y. Chen, Y. Zhang, Y. Wang, C. Sun and C. Zhang, *J. Appl. Polym. Sci.*, 2013, **127**, 1485–1492; (c) Y.-N. Zhou, J.-J. Li and Z.-H. Luo, *J. Polym. Sci., Part A: Polym. Chem.*, 2012, **50**, 3052–3066; (d) Y. Milonaki, E. Kaditi, S. Pispas and C. Demetzos, *J. Polym. Sci., Part A: Polym. Chem.*, 2012, **50**, 1226–1237.
- For examples of semicrystalline gradient copolymer synthesis, see: (a) E. F. Palermo and A. J. McNeil, *Macromolecules*, 2012, **45**, 5948–5955; (b) J. R. Locke and A. J. McNeil, *Macromolecules*, 2010, **43**, 8709–8710.
- (a) D. Sun and H. Guo, *J. Phys. Chem. B*, 2012, **116**, 9512–9522; (b) R. Malik, C. K. Hall and J. Genzer, *Soft Matter*, 2011, **7**, 10620–10630; (c) J. Kim, R. W. Sandoval, C. M. Dettmer, S. T. Nguyen and J. M. Torkelson, *Polymer*, 2008, **49**, 2686–2697; (d) Y. Tao, J. Kim and J. M. Torkelson, *Polymer*, 2006, **47**, 6773–6781; (e) J. Kim, H. Zhou, S. T. Nguyen and J. M. Torkelson, *Polymer*, 2006, **47**, 5799–5809; (f) J. Kim, M. K. Gray, H. Zhou, S. T. Nguyen and J. M. Torkelson, *Macromolecules*, 2005, **38**, 1037–1040.
- For leading references, see: (a) W. Chen, M. P. Nikiforov and S. B. Darling, *Energy Environ. Sci.*, 2012, **5**, 8045–8074; (b) M. A. Brady, G. M. Su and M. L. Chabinye, *Soft Matter*, 2011, **7**, 11065–11077; (c) C. J. Brabec, M. Heeney, I. McCullough and J. Nelson, *Chem. Soc. Rev.*, 2011, **40**, 1185–1199.
- Blends of poly(alkylthiophene)s with different side-chain lengths can show phase separation. For references, see: (a) Y. Qu, L. Li, G. Lu, X. Zhou, Q. Su, W. Xu, S. Li, J. Zhang and X. Yang, *Polym. Chem.*, 2012, **3**, 3301–3307; (b) S. Pal

- and A. K. Nandi, *J. Phys. Chem. B*, 2005, **109**, 2493–2498; (c) S. Pal and A. K. Nandi, *Macromolecules*, 2003, **36**, 8426–8432.
- 9 A. Marrocchi, D. Lanari, A. Facchetti and L. Vaccaro, *Energy Environ. Sci.*, 2012, **5**, 8457–8474.
- 10 (a) A. Yokoyama, R. Miyakoshi and T. Yokozawa, *Macromolecules*, 2004, **37**, 1169–1171; (b) R. Miyakoshi, A. Yokoyama and T. Yokozawa, *Macromol. Rapid Commun.*, 2004, **25**, 1663–1666; (c) E. E. Sheina, J. S. Liu, M. C. Iovu, D. W. Laird and R. D. McCullough, *Macromolecules*, 2004, **37**, 3526–3528.
- 11 For recent reviews, see: (a) T. Yokozawa, Y. Nanashima and Y. Ohta, *ACS Macro Lett.*, 2012, **1**, 862–866; (b) A. J. McNeil and E. L. Lanni, *New Conjugated Polymers and Synthetic Methods*, in *Synthesis of Polymers*, ed. D. A. Schlüter, C. J. Hawker and J. Sakamoto, Wiley-VCH, Germany, 2012, vol. 1, pp. 475–486; (c) A. Kiriy, V. Senkovskyy and M. Sommer, *Macromol. Rapid Commun.*, 2011, **32**, 1503–1517.
- 12 Some details of chain-growth mechanism remain highly debated. For leading references, see: (a) Z. J. Bryan and A. J. McNeil, *Chem. Sci.*, 2013, **4**, 1620–1624; (b) S. R. Lee, Z. J. Bryan, A. M. Wagner and A. J. McNeil, *Chem. Sci.*, 2012, **3**, 1562–1566; (c) V. Senkovskyy, R. Tkachov, H. Komber, A. John, J.-U. Sommer and A. Kiriy, *Macromolecules*, 2012, **45**, 7770–7777.
- 13 For recent examples, see: (a) M. Yuan, K. Okamoto, H. A. Bronstein and C. K. Luscombe, *ACS Macro Lett.*, 2012, **1**, 392–395; (b) V. Senkovskyy, T. Beryozkina, V. Bocharova, R. Tkachov, H. Komber, A. Lederer, M. Stamm, N. Severin, J. P. Rabe and A. Kiriy, *Macromol. Symp.*, 2010, **291–292**, 17–25.
- 14 For recent examples, see: (a) N. Doubina, J. L. Jenkins, S. A. Paniagua, K. A. Mazzio, G. A. MacDonald, A. K. Y. Jen, N. R. Armstrong, S. R. Marder and C. K. Luscombe, *Langmuir*, 2012, **28**, 1900–1908; (b) N. E. Huddleston, S. K. Sontag, J. A. Bilbrey, G. R. Sheppard and J. Locklin, *Macromol. Rapid Commun.*, 2012, **33**, 2115–2120; (c) L. Q. Yang, S. K. Sontag, T. W. Lajoie, W. T. Li, N. E. Huddleston, J. Locklin and W. You, *ACS Appl. Mater. Interfaces*, 2012, **4**, 5069–5073; (d) N. Marshall, S. K. Sontag and J. Locklin, *Chem. Commun.*, 2011, **47**, 5681–5689.
- 15 L. Zhai, R. L. Pilston, K. L. Zaiger, K. K. Stokes and R. D. McCullough, *Macromolecules*, 2003, **36**, 61–64.
- 16 X. Wu, T.-A. Chen, L. Zhu and R. D. Rieke, *Tetrahedron Lett.*, 1994, **35**, 3673–3674.
- 17 E. L. Lanni and A. J. McNeil, *J. Am. Chem. Soc.*, 2009, **131**, 16573–16579.
- 18 (a) P. Kohn, S. Huettner, H. Komber, V. Senkovskyy, R. Tkachov, A. Kiriy, R. H. Friend, U. Steiner, W. T. S. Huck, J.-U. Sommer and M. Sommer, *J. Am. Chem. Soc.*, 2012, **134**, 4790–4805; (b) H. Komber, V. Senkovskyy, R. Tkachov, K. Johnson, A. Kiriy, W. T. S. Huck and M. Sommer, *Macromolecules*, 2011, **44**, 9164–9172; (c) R. Tkachov, V. Senkovskyy, H. Komber, J. U. Sommer and A. Kiriy, *J. Am. Chem. Soc.*, 2010, **132**, 7803–7810.
- 19 The MALDI spectrum of oligo(3BrHT) showed a minor series of peaks corresponding to tolyl/H-terminated polymer minus 80 *m/z* units. Because these peaks were suppressed when the laser power was decreased, we suspected some C–Br fragmentation occurs during the ionization process. For reference, see: J. Liu, R. S. Loewe and R. D. McCullough, *Macromolecules*, 1999, **32**, 5777–5785.
- 20 Thin films of P3HT and P3BrHT were annealed at 220 and 150 °C, respectively. If P3BrHT was annealed at higher temperatures, an insoluble material was produced that we suspect results from homolytic cleavage of the C–Br bond and subsequent crosslinking with the polymer backbone.
- 21 (a) J. Clark, J.-F. Chang, F. C. Spano, R. H. Friend and C. Silva, *Appl. Phys. Lett.*, 2009, **94**, 163306; (b) J. Gierschner, Y.-S. Huang, B. Van Averbeke, J. Cornil, R. H. Friend and D. J. Beljonne, *Chem. Phys.*, 2009, **130**, 044105; (c) J. Clark, C. Silva, R. H. Friend and F. C. Spano, *Phys. Rev. Lett.*, 2007, **98**, 206406; (d) P. J. Brown, D. S. Thomas, A. Köhler, J. S. Wilson, J.-S. Kim, C. M. Ramsdale, H. Sirringhaus and R. H. Friend, *Phys. Rev. B: Condens. Matter Mater. Phys.*, 2003, **67**, 064203; (e) F. C. Spano, *Acc. Chem. Res.*, 2010, **43**, 429–439.
- 22 For references, see: (a) K. Tashiro, M. Kobayashi, T. Kawai and K. Yoshino, *Polymer*, 1997, **38**, 2867–2879; (b) R. D. McCullough, S. Tristram-Nagle, S. P. Williams, R. D. Lowe and M. Jayaraman, *J. Am. Chem. Soc.*, 1993, **115**, 4910–4911.
- 23 This comparison takes into account the known overestimation of molecular weight (~1.5×) when using polystyrene standards. For a recent example, see: M. Wong, J. Hollinger, L. M. Kozycz, T. M. McCormick, Y. J. Lu, D. C. Burns and D. S. Seferos, *ACS Macro Lett.*, 2012, **1**, 1266–1269.
- 24 (a) J.-U. Sommer and C. Luo, *J. Polym. Sci., Part B: Polym. Phys.*, 2010, **48**, 2222–2232; (b) C. Luo and J.-U. Sommer, *Phys. Rev. Lett.*, 2009, **102**, 147801.
- 25 The copolymer films were thermally annealed in a vacuum oven at 150 °C before the UV/vis spectra were acquired.
- 26 C. R. McNeill, *Energy Environ. Sci.*, 2012, **5**, 5653–5667.